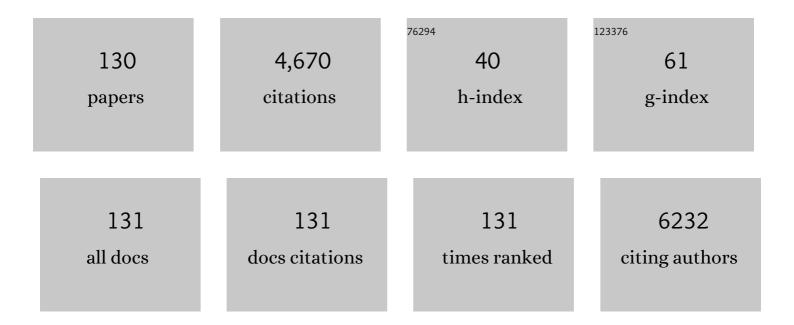
Abbas Ali Khodadadi

List of Publications by Year in descending order

Source: https://exaly.com/author-pdf/3080622/publications.pdf Version: 2024-02-01



#	Article	IF	CITATIONS
1	Enhanced NO 2 gas sensing performance of bare and Pd-loaded SnO 2 thick film sensors under UV-light irradiation at room temperature. Sensors and Actuators B: Chemical, 2016, 223, 429-439.	4.0	174
2	Asphaltene Adsorption onto Acidic/Basic Metal Oxide Nanoparticles toward in Situ Upgrading of Reservoir Oils by Nanotechnology. Langmuir, 2013, 29, 14135-14146.	1.6	165
3	Fast and clean functionalization of carbon nanotubes by dielectric barrier discharge plasma in air compared to acid treatment. Carbon, 2010, 48, 1369-1379.	5.4	133
4	Highly active Fe2O3-doped TiO2 photocatalyst for degradation of trichloroethylene in air under UV and visible light irradiation: Experimental and computational studies. Applied Catalysis B: Environmental, 2015, 165, 209-221.	10.8	117
5	Microwave assisted fast synthesis of various ZnO morphologies for selective detection of CO, CH4 and ethanol. Sensors and Actuators B: Chemical, 2011, 156, 737-742.	4.0	108
6	Highly sensitive carbon nanotubes–SnO2 nanocomposite sensor for acetone detection in diabetes mellitus breath. Sensors and Actuators B: Chemical, 2014, 205, 261-267.	4.0	104
7	Stability and thermal conductivity of nanofluids of tin dioxide synthesized via microwave-induced combustion route. Chemical Engineering Journal, 2010, 156, 471-478.	6.6	97
8	Cerium oxide/SnO2-based semiconductor gas sensors with improved sensitivity to CO. Sensors and Actuators B: Chemical, 2001, 80, 267-271.	4.0	88
9	Ultra-deep adsorptive desulfurization of a model diesel fuel on regenerable Ni–Cu/γ-Al2O3 at low temperatures in absence of hydrogen. Journal of Hazardous Materials, 2014, 271, 120-130.	6.5	88
10	Nanostructured SnO2–ZnO sensors: Highly sensitive and selective to ethanol. Sensors and Actuators B: Chemical, 2011, 160, 1298-1303.	4.0	86
11	Targeted Delivery of Docetaxel by Use of Transferrin/Poly(allylamine hydrochloride)-functionalized Graphene Oxide Nanocarrier. ACS Applied Materials & Interfaces, 2016, 8, 13282-13293.	4.0	83
12	Single-wall carbon nanotubes synthesized using organic additives to Co–Mo catalysts supported on nanoporous MgO. Nanotechnology, 2007, 18, 315605.	1.3	80
13	Enhanced pyrolysis and oxidation of asphaltenes adsorbed onto transition metal oxides nanoparticles towards advanced in-situ combustion EOR processes by nanotechnology. Applied Catalysis A: General, 2014, 477, 159-171.	2.2	76
14	Alkaline- and template-free hydrothermal synthesis of stable SnO2 nanoparticles and nanorods for CO and ethanol gas sensing. Sensors and Actuators B: Chemical, 2010, 151, 140-145.	4.0	75
15	CeO2 doped ZnO flower-like nanostructure sensor selective to ethanol in presence of CO and CH4. Sensors and Actuators B: Chemical, 2012, 169, 67-73.	4.0	75
16	Highly sensitive and selective ethanol sensor based on Sm2O3-loaded flower-like ZnO nanostructure. Sensors and Actuators B: Chemical, 2014, 191, 283-290.	4.0	75
17	A functionalized nano-structured cellulosic sorbent aerogel for oil spill cleanup: Synthesis and characterization. Journal of Hazardous Materials, 2019, 366, 229-239.	6.5	75
18	Highly sensitive CO and ethanol nanoflower-like SnO2 sensor among various morphologies obtained by using single and mixed ionic surfactant templates. Sensors and Actuators B: Chemical, 2009, 141, 89-96.	4.0	74

#	Article	IF	CITATIONS
19	Highly sensitive and selective ethanol and acetone gas sensors by adding some dopants (Mn, Fe, Co, Ni) onto hexagonal ZnO plates. RSC Advances, 2016, 6, 7838-7845.	1.7	73
20	CO and ethanol dual selective sensor of Sm2O3-doped SnO2 nanoparticles synthesized by microwave-induced combustion. Sensors and Actuators B: Chemical, 2010, 144, 131-138.	4.0	72
21	Effects of Pd on enhancement of oxidation activity of LaBO3 (B=Mn, Fe, Co and Ni) pervoskite catalysts for pollution abatement from natural gas fueled vehicles. Applied Catalysis B: Environmental, 2011, 102, 62-70.	10.8	72
22	Kinetic modeling of oxidative coupling of methane over Mn/Na2WO4/SiO2 catalyst. Fuel Processing Technology, 2009, 90, 403-410.	3.7	69
23	Preparation of SnO2 nanoparticles and nanorods by using a hydrothermal method at low temperature. Materials Letters, 2008, 62, 1789-1792.	1.3	68
24	Synthesis and gas-sensing properties of nano- and meso-porous MoO3-doped SnO2. Sensors and Actuators B: Chemical, 2010, 147, 554-560.	4.0	66
25	Highly sensitive and selective sensors to volatile organic compounds using MWCNTs/SnO2. Sensors and Actuators B: Chemical, 2012, 166-167, 150-155.	4.0	66
26	Thermal and rheological properties improvement of drilling fluids using functionalized carbon nanotubes. Applied Nanoscience (Switzerland), 2015, 5, 651-659.	1.6	62
27	Targeting graphene quantum dots to epidermal growth factor receptor for delivery of cisplatin and cellular imaging. Materials Science and Engineering C, 2019, 94, 247-257.	3.8	58
28	Synergetic effects of plasma and metal oxide catalysts on diesel soot oxidation. Applied Catalysis B: Environmental, 2016, 182, 74-84.	10.8	57
29	In2O3–ZnO nanocomposites: High sensor response and selectivity to ethanol. Sensors and Actuators B: Chemical, 2015, 212, 395-403.	4.0	55
30	Pd-doped LaCoO3 regenerative catalyst for automotive emissions control. Applied Catalysis B: Environmental, 2008, 83, 214-220.	10.8	53
31	Sm2O3 doped-SnO2 nanoparticles, very selective and sensitive to volatile organic compounds. Sensors and Actuators B: Chemical, 2013, 181, 910-918.	4.0	53
32	Highly sensitive and selective Gd2O3-doped SnO2 ethanol sensors synthesized by a high temperature and pressure solvothermal method in a microreactor. Sensors and Actuators B: Chemical, 2016, 230, 130-139.	4.0	53
33	Highly enhanced response and selectivity of electrospun ZnO-doped SnO2 sensors to ethanol and CO in presence of CH4. Sensors and Actuators B: Chemical, 2013, 184, 196-204.	4.0	51
34	High photocatalytic activity of Zn2SnO4 among various nanostructures of Zn2xSn1â^'xO2 prepared by a hydrothermal method. Chemical Engineering Journal, 2010, 165, 735-739.	6.6	49
35	Effects of excess manganese in lanthanum manganite perovskite on lowering oxidation light-off temperature for automotive exhaust gas pollutants. Chemical Engineering Journal, 2011, 169, 282-289.	6.6	48
36	Effects of alumina phases as nickel supports on deep reactive adsorption of (4,6-dimethyl) dibenzothiophene: Comparison between γ, δ, and Î, alumina. Applied Catalysis B: Environmental, 2016, 180, 312-323.	10.8	47

#	Article	IF	CITATIONS
37	The sensing behaviour of metal oxides (ZnO, CuO and Sm2O3) doped-SnO2 for detection of low concentrations of chlorinated volatile organic compounds. Sensors and Actuators B: Chemical, 2013, 181, 637-643.	4.0	42
38	Highly Stable and Selective Non-Enzymatic Glucose Biosensor Using Carbon Nanotubes Decorated by Fe3O4Nanoparticles. Journal of the Electrochemical Society, 2014, 161, B19-B25.	1.3	42
39	Enhanced methanol electro-oxidation activity of Pt/MWCNTs electro-catalyst using manganese oxide deposited on MWCNTs. Electrochimica Acta, 2014, 147, 192-200.	2.6	42
40	Ru promoted cobalt catalyst on γ-Al2O3: Influence of different catalyst preparation method and Ru loadings on Fischer–Tropsch reaction and kinetics. Applied Surface Science, 2014, 313, 183-195.	3.1	42
41	Atomic layer deposited Co/γ-Al2O3 catalyst with enhanced cobalt dispersion and Fischer–Tropsch synthesis activity and selectivity. Applied Catalysis A: General, 2016, 511, 31-46.	2.2	42
42	Enormous enhancement of Pt/SnO2 sensors response and selectivity by their reduction, to CO in automotive exhaust gas pollutants including CO, NOx and C3H8. Applied Surface Science, 2021, 546, 149120.	3.1	42
43	A Glucose Biosensor Based on Glucose Oxidase Immobilized on ZnO/Cu ₂ O Graphene Oxide Nanocomposite Electrode. Journal of the Electrochemical Society, 2014, 161, B81-B87.	1.3	41
44	Apple – biomorphic synthesis of porous ZnO nanostructures for glucose direct electrochemical biosensor. Current Applied Physics, 2012, 12, 1033-1038.	1.1	40
45	Effects of flower-like, sheet-like and granular SnO2 nanostructures prepared by solid-state reactions on CO sensing. Materials Chemistry and Physics, 2009, 115, 196-199.	2.0	39
46	Highly selective Pt/SnO2 sensor to propane or methane in presence of CO and ethanol, using gold nanoparticles on Fe2O3 catalytic filter. Sensors and Actuators B: Chemical, 2010, 147, 400-405.	4.0	38
47	The effects of excess manganese in nano-size lanthanum manganite perovskite on enhancement of trichloroethylene oxidation activity. Chemical Engineering Journal, 2013, 215-216, 827-837.	6.6	38
48	A cost-effective strategy for marine microalgae separation by electro-coagulation–flotation process aimed at bio-crude oil production: Optimization and evaluation study. Separation and Purification Technology, 2015, 147, 156-165.	3.9	38
49	Dual selective Pt/SnO2 sensor to CO and propane in exhaust gases of gasoline engines using Pt/LaFeO3 filter. Sensors and Actuators B: Chemical, 2015, 206, 617-623.	4.0	37
50	Effect of α-Fe2O3 addition on the morphological, optical and decolorization properties of ZnO nanostructures. Materials Chemistry and Physics, 2012, 133, 311-316.	2.0	35
51	Nano-ceria–zirconia promoter effects on enhanced coke combustion and oxidation of CO formed in regeneration of silica–alumina coked during cracking of triisopropylbenzene. Applied Catalysis A: General, 2009, 353, 271-281.	2.2	34
52	Microemulsion synthesized silica/ZnO stable core/shell sensors highly selective to ethanol with minimum sensitivity to humidity. Sensors and Actuators B: Chemical, 2017, 238, 1070-1083.	4.0	34
53	Glucosamine-conjugated graphene quantum dots as versatile and pH-sensitive nanocarriers for enhanced delivery of curcumin targeting to breast cancer. Materials Science and Engineering C, 2021, 121, 111809.	3.8	34
54	Highly sensitive gallia-SnO2 nanocomposite sensors to CO and ethanol in presence of methane. Sensors and Actuators B: Chemical, 2013, 188, 45-52.	4.0	32

#	Article	IF	CITATIONS
55	Vanadium oxide decorated carbon nanotubes as a promising support of Pt nanoparticles for methanol electro-oxidation reaction. Journal of Colloid and Interface Science, 2013, 393, 291-299.	5.0	31
56	Facile surface functionalization of multiwalled carbon nanotubes by soft dielectric barrier discharge plasma: Generate compatible interface for lipase immobilization. Biochemical Engineering Journal, 2014, 90, 16-26.	1.8	31
57	A hydrophobic/oleophilic chitosan-based sorbent: Toward an effective oil spill remediation technology. Journal of Environmental Chemical Engineering, 2019, 7, 103340.	3.3	30
58	Oxygen sensor with solid-state CeO2–ZrO2–TiO2 reference. Sensors and Actuators B: Chemical, 2005, 108, 341-345.	4.0	29
59	Tube fitted bulk monolithic catalyst as novel structured reactor for gas–solid reactions. Applied Catalysis A: General, 2010, 385, 214-223.	2.2	29
60	Artificial intelligence modeling of DME conversion to gasoline and light olefins over modified nano ZSM-5 catalysts. Fuel, 2016, 179, 79-86.	3.4	29
61	An yttria-doped ceria-based oxygen sensor with solid-state reference. Sensors and Actuators B: Chemical, 2004, 103, 178-183.	4.0	28
62	The role of tin-promoted Pd/MWNTs via the management of carbonaceous species in selective hydrogenation of high concentration acetylene. Applied Surface Science, 2012, 263, 513-522.	3.1	28
63	Coupled Metal Oxide-Doped Pt/SnO ₂ Semiconductor and Yittria-Stabilized Zirconia Electrochemical Sensors for Detection of VOCs. Journal of the Electrochemical Society, 2013, 160, B218-B224.	1.3	28
64	Strong effects of gallia on structure and selective responses of Ga2O3–In2O3 nanocomposite sensors to either ethanol, CO or CH4. Sensors and Actuators B: Chemical, 2015, 220, 590-599.	4.0	28
65	Functionalized MWCNTs effects on dramatic enhancement of MWCNTs/SnO 2 nanocomposite gas sensing properties at low temperatures. Sensors and Actuators B: Chemical, 2016, 223, 252-260.	4.0	28
66	Enhanced catalytic performance of Au/CuO–ZnO catalysts containing low CuO content for preferential oxidation of carbon monoxide in hydrogen-rich streams for PEMFC. International Journal of Hydrogen Energy, 2014, 39, 2056-2066.	3.8	27
67	Preferential chemical vapor deposition of ruthenium on cobalt with highly enhanced activity and selectivity for Fischer–Tropsch synthesis. Applied Catalysis A: General, 2014, 470, 221-231.	2.2	25
68	A simple method for blocking defects in zeolite membranes. Journal of Membrane Science, 2015, 489, 270-274.	4.1	25
69	Gallia–ZnO nanohybrid sensors with dramatically higher sensitivity to ethanol in presence of CO, methane and VOCs. Sensors and Actuators B: Chemical, 2016, 223, 576-585.	4.0	25
70	Plasma Functionalization of MWCNTs in He Followed by NH ₃ Treatment and its Application in PMMA Based Nanocomposites. Plasma Processes and Polymers, 2010, 7, 1001-1009.	1.6	24
71	Palladium–Tin nanocatalysts in high concentration acetylene hydrogenation: A novel deactivation mechanism. Fuel Processing Technology, 2014, 120, 113-122.	3.7	24
72	H ₂ 0/air plasma-functionalized carbon nanotubes decorated with MnO ₂ for glucose sensing. RSC Advances, 2016, 6, 31807-31815.	1.7	24

Abbas Ali Khodadadi

#	Article	IF	CITATIONS
73	Fast photocatalytic degradation of congo red using CoO-doped β-Ga ₂ O ₃ nanostructures. RSC Advances, 2014, 4, 33262-33268.	1.7	23
74	SnO 2 decorated SiO 2 chemical sensors: Enhanced sensing performance toward ethanol and acetone. Materials Science in Semiconductor Processing, 2017, 68, 87-96.	1.9	22
75	Co-pyrolysis of municipal sewage sludge and microalgae Chlorella Vulgaris: Products' optimization; thermo-kinetic study, and ANN modeling. Energy Conversion and Management, 2022, 254, 115258.	4.4	22
76	Effect of partial substitution of lanthanum by strontium or bismuth on structural features of the lanthanum manganite nanoparticles as a catalyst for carbon monoxide oxidation. Catalysis Communications, 2012, 28, 32-37.	1.6	21
77	Understanding the mechanism of synthesis of Pt ₃ Co intermetallic nanoparticles <i>via</i> preferential chemical vapor deposition. Journal of Materials Chemistry A, 2017, 5, 24396-24406.	5.2	21
78	Effects of nanoadditives on stability of Pt/SnO2 as a sensing material for detection of CO. Sensors and Actuators B: Chemical, 2014, 191, 421-430.	4.0	19
79	Plasma Functionalized Multiwalled Carbon Nanotubes for Immobilization of Candida antarctica Lipase B: Production of Biodiesel from Methanolysis of Rapeseed Oil. Applied Biochemistry and Biotechnology, 2016, 178, 974-989.	1.4	19
80	Enhanced methanol electro-oxidation reaction on Pt-CoOx/MWCNTs hybrid electro-catalyst. Applied Surface Science, 2015, 335, 55-64.	3.1	18
81	Modeling the Growth of Carbon Nanotubes in a Floating Catalyst Reactor. Industrial & Engineering Chemistry Research, 2012, 51, 1143-1149.	1.8	17
82	Functionalization of silica membranes for CO2 separation. Separation and Purification Technology, 2020, 235, 116207.	3.9	17
83	Asphaltene Adsorption onto Carbonaceous Nanostructures. Energy & amp; Fuels, 2020, 34, 211-224.	2.5	17
84	Detailed profiling of CNTs arrays along the growth window in a floating catalyst reactor. Applied Surface Science, 2009, 255, 7243-7250.	3.1	16
85	Novel Microwave-Induced Combustion Synthesis of SnO ₂ Nanoparticles for Selective Sensing of CO Using Tin Chloride. Journal of Nanoscience and Nanotechnology, 2010, 10, 6003-6008.	0.9	16
86	Plasma thiol-functionalized carbon nanotubes decorated with gold nanoparticles for glucose biosensor. Sensors and Actuators B: Chemical, 2013, 188, 488-495.	4.0	16
87	High flux acetate functionalized silica membranes based on in-situ co-condensation for CO2/N2 separation. Journal of Membrane Science, 2016, 520, 574-582.	4.1	16
88	Characteristics and performance of urea modified Pt-MWCNTs for electro-oxidation of methanol. Applied Surface Science, 2019, 467-468, 335-344.	3.1	16
89	Au-promoted Ce-Zr catalytic filter for Pt/SnO2 sensor to selectively detect methane and ethanol in the presence of interfering indoor gases. Materials Science in Semiconductor Processing, 2019, 90, 182-189.	1.9	15
90	A novel biosensor using entangled carbon nanotubes layer grown on an alumina substrate by CCVD of methane on FeOx–MgO. Sensors and Actuators B: Chemical, 2009, 141, 526-531.	4.0	14

Abbas Ali Khodadadi

#	Article	IF	CITATIONS
91	Effect of mass transfer limitations on catalyst performance during reduction and carburization of iron based Fischer-Tropsch synthesis catalysts. Journal of Energy Chemistry, 2013, 22, 795-803.	7.1	14
92	Vapor-phase selective o-alkylation of catechol with methanol over lanthanum phosphate and its modified catalysts with Ti and Cs. Journal of Molecular Catalysis A, 2013, 372, 79-83.	4.8	14
93	Experimental and theoretical study of CO adsorption on the surface of single phase hexagonally plate ZnO. Applied Surface Science, 2014, 315, 8-15.	3.1	14
94	Cumene cracking activity and enhanced regeneration of FCC catalysts comprising HY-zeolite and LaBO 3 (B = Co, Mn, and Fe) perovskites. Applied Catalysis A: General, 2014, 487, 26-35.	2.2	14
95	Effects of Combustion Catalyst Dispersed by a Novel Microemulsion Method as Fuel Additive on Diesel Engine Emissions, Performance, and Characteristics. Energy & Fuels, 2016, 30, 3392-3402.	2.5	14
96	Modeling of Stagewise Feeding in Fluidized Bed Reactor of Oxidative Coupling of Methane. Energy & Fuels, 2009, 23, 3745-3752.	2.5	13
97	Facile ultrasonic-assisted synthesis of SiO2/ZnO core/shell nanostructures: A selective ethanol sensor at low temperatures with enhanced recovery. Sensors and Actuators B: Chemical, 2022, 368, 132187.	4.0	13
98	Ultra-low Electrical and Rheological Percolation Thresholds in PMMA/Plasma-Functionalized CNTs Nanocomposites. Polymer-Plastics Technology and Engineering, 2014, 53, 1450-1455.	1.9	12
99	Functionalized open-ended vertically aligned carbon nanotube composite membranes with high salt rejection and enhanced slip flow for desalination. Separation and Purification Technology, 2021, 279, 119773.	3.9	12
100	Comparative model analysis of the performance of tube fitted bulk monolithic catalyst with conventional pellet shapes for natural gas reforming. Journal of Industrial and Engineering Chemistry, 2011, 17, 767-776.	2.9	11
101	Rapid and enhanced functionalization of MWCNTs in a dielectric barrier discharge plasma in presence of diluted CO2. Applied Physics A: Materials Science and Processing, 2012, 106, 829-836.	1.1	11
102	On the dispersion of CNTs in polyamide 6 matrix via solution methods: assessment through electrical, rheological, thermal and morphological analyses. Polymer Bulletin, 2013, 70, 2387-2398.	1.7	11
103	Nano-structured Pd doped LaFe(Co)O3 perovskite; synthesis, characterization and catalytic behavior. Materials Chemistry and Physics, 2018, 205, 228-239.	2.0	11
104	SMFs-supported Pd nanocatalysts in selective acetylene hydrogenation: Pore structure-dependent deactivation mechanism. Journal of Energy Chemistry, 2013, 22, 717-725.	7.1	10
105	Two-stage cracking catalyst of amorphous silica-alumina on Y zeolite for enhanced product selectivity and suppressed coking. Korean Journal of Chemical Engineering, 2017, 34, 681-691.	1.2	10
106	Application of cobalt oxide nanoparticles as an electron transfer facilitator in direct electron transfer and biocatalytic reactivity of cytochrome c. Journal of Applied Electrochemistry, 2011, 41, 115-121.	1.5	9
107	Direct electron transfer and biocatalytic activity of iron storage protein molecules immobilized on electrodeposited cobalt oxide nanoparticles. Mikrochimica Acta, 2011, 173, 317-322.	2.5	9
108	High performance Ni–CNTs catalyst: synthesis and characterization. RSC Advances, 2016, 6, 47072-47082.	1.7	9

#	Article	IF	CITATIONS
109	Atmospheric pressure atomic layer deposition of iron oxide nanolayer on the Al2O3/SiO2/Si substrate for mm-tall vertically aligned CNTs growth. Journal of Materials Science, 2020, 55, 13634-13657.	1.7	9
110	Effects of ceria addition and pre-calcination temperature on performance of cobalt catalysts for Fischer-Tropsch synthesis. Reaction Kinetics and Catalysis Letters, 2006, 88, 225-232.	0.6	8
111	Acetic acid effects on enhancement of growth rate and reduction of amorphous carbon deposition on CNT arrays along a growth window in a floating catalyst reactor. Applied Physics A: Materials Science and Processing, 2009, 97, 417-424.	1.1	8
112	Highly Sensitive Tin Oxide Hollow Microspheres and Nanosheets to Ethanol Gas Prepared by Hydrothermal Method. Journal of Nanoscience and Nanotechnology, 2010, 10, 6049-6055.	0.9	8
113	Self-regenerative function of Cu in LaMnCu0.1O3 catalyst: Towards noble metal-free intelligent perovskites for automotive exhaust gas treatment. Applied Catalysis A: General, 2020, 602, 117702.	2.2	8
114	Tuning the band-gap and enhancing the trichloroethylene photocatalytic degradation activities of flower-like Ni-doped SnS2/SnO2 heterostructures by partial oxidation. Journal of Environmental Chemical Engineering, 2022, 10, 107793.	3.3	8
115	Highly efficient MoO2.5(OH)0.5-doped ZnO nanoflower for photodecolorization of azo dye. Solid State Sciences, 2013, 26, 9-15.	1.5	7
116	Combination of Plasma Functionalization and Phase Inversion Process Techniques for Efficient Dispersion of MWCNTs in Polyamide 6: Assessment through Morphological, Electrical, Rheological and Thermal Properties. Polymer-Plastics Technology and Engineering, 2015, 54, 632-638.	1.9	6
117	Cyclic molecular designed dispersion (CMDD) of Fe2O3 on CeO2 promoted by Au for preferential CO oxidation in hydrogen. International Journal of Hydrogen Energy, 2020, 45, 33598-33611.	3.8	6
118	Anomalous low–high transition of ceria doped SnO sensors exposed to synthetic automobile exhaust gas. Sensors and Actuators B: Chemical, 2005, 106, 816-822.	4.0	5
119	Dry Reforming of Methane over Ni/ <i>γ</i> â€MgO Catalysts in a Coaxial Dielectric Barrier Discharge Reactor. Chemical Engineering and Technology, 2021, 44, 589-599.	0.9	5
120	Fabrication and Highly Sensitive Gas Sensors Based on h-MoO ₃ /SnO ₂ Hollow Nanostructures Operated at Low Temperatures. Journal of Nanoscience and Nanotechnology, 2010, 10, 6155-6160.	0.9	4
121	The effects of carrier gas and liquid feed flow rates on longitudinal patterns of CNT growth. Materials Chemistry and Physics, 2010, 124, 1139-1145.	2.0	4
122	Effects of nitrogen-containing functional groups of reduced graphene oxide as a support for Pd in selective hydrogenation of cinnamaldehyde. Research on Chemical Intermediates, 2021, 47, 1429-1446.	1.3	4
123	In-situ one-step deposition of highly dispersed palladium nanoparticles into zirconium metal–organic framework for selective hydrogenation of furfural. Molecular Catalysis, 2021, 514, 111859.	1.0	4
124	A Comparison of a Nanostructured Enzymeless Au/Fe ₂ O ₃ /MWCNTs/GCE Electrode and a GOx Modified One in Electrocatalytic Detection of Glucose. Electroanalysis, 2018, 30, 2044-2052.	1.5	3
125	Selective detection of unburned-hydrocarbon in the exhaust gas using catalytic filter. , 2014, , .		2
126	Highly dispersed atomic layer deposited CrOx on SiO2 catalyst with enhanced yield of propylene for CO2 –mediated oxidative dehydrogenation of propane. Molecular Catalysis, 2022, 526, 112396.	1.0	2

#	Article	IF	CITATIONS
127	Oxidative Coupling of Methane in a Negative DC Corona Reactor at Low Temperature. Canadian Journal of Chemical Engineering, 2003, 81, 37-42.	0.9	1
128	Preferential Oxidation of CO Based on Electro-Thermally Assisted Catalytic Ni/Cu Nanostructures on Si Micro-Grass. ECS Transactions, 2011, 35, 37-41.	0.3	0
129	Simultaneous Effect of the Catalyst Precursor Concentration and the Longitudinal Position on the Growth Patterns of Multiwalled Carbon Nanotubes. Industrial & Engineering Chemistry Research, 2014, 53, 1293-1300.	1.8	0
130	Recognition of Oxidative Coupling of Methane Reactor Performance Patterns. Chemical Engineering and Technology, 0, , .	0.9	0